Math. Nachr. **280,** No. 13–14, 1577 – 1594 (2007) / **DOI** 10.1002/mana.200410566

An interface problem for a Sierpinski and a Vicsek fractal

Volker Metz[*1] and **Peter Grabner**[**2]

[1] Bielefeld University, 33501 Bielefeld, Germany
[2] Institute of Mathematics A, Graz University of Technology, Steyrergasse 30, 8010 Graz, Austria

Received 29 December 2004, revised 28 October 2005, accepted 27 January 2006
Published online 6 September 2007

Key words Laplace operator, Brownian motion, interface, fractals
MSC (2000) 31C25, 60J45, 80A28

We suggest a flexible way to study the self-similar interface of two different fractals. In contrast to previous methods the participating energies are modified in the neighborhood of the intersection of the fractals. In the example of the Vicsek snowflake and the 3-gasket, a variant of the Sierpinski gasket, we calculate the admissible transition constants via the "Short-cut Test". The resulting range of values is reinterpreted in terms of traces of Lipschitz spaces on the intersection. This allows us to describe the interface effects of different transition constants and indicates the techniques necessary to generalize the present interface results.

1 Introduction and results

In 1993 Lindstrøm was the first to embed a fractal, the Sierpinski gasket, into the Euclidean plane and connect them [20]. Later on Kumagai, Jonsson and Hambly/Kumagai extended his work by analytical means [17, 12, 9]. They identified the domain of the fractal Dirichlet form as a certain Lipschitz space and used an extension map of Jonsson and Wallin, [14], to extend these functions to the plane. Then they verified that sufficiently many of them lie in the domain of the plane Laplacian. In other words, the transition can be defined by superimposing the two component Laplacians on the interface, and transition across the interface takes place in both directions. This type of connection might be called "instantaneous transition", because the composite Laplacian coincides with the respective component Laplacians outside the overlap of the two media. When the plane is replaced by some other fractal, the Lipschitz functions of the plane have to be extended to the fractals.

To avoid such technicalities and for engineering reasons we want to suggest a different form of transition which might be called "gradual transition", because the two media in question are changed gradually into a medium which allows transition. The character of this connection can be modified in choosing a transition constant η_C in a certain interval. The region in which the original media have to be changed is necessarily of positive Hausdorff measure. This approach has two advantages: (1) When the union of the component fractals is still self-similar, then the interface also is, that is, the composite Dirichlet form has a self-similar scaling. (2) Physically, the two connected media influence each other (possibly on a molecular scale) in a small neighborhood of the interface. Because of the self-similarity, the rescaling can be performed exclusively on this neighborhood. The disadvantage of our setup is the self-similar interface, that is, an unusually nice match of the participating structures. For this reason the present paper can only provide two detailed case studies, the house and the thumbtack fractal. Hopefully, the detailed effects described below will stimulate further research.

The main results of this paper are the Theorems 6.5, 6.6 and 7.3. In the first two those transition weights are identified which guarantee a self-similar continuous transport across the interface of our composite models in both directions. The range of admissible transition weights is surprisingly large. The lower bound is a consequence of the fact that points should have positive capacity and the upper bound implies a finite conductivity of the interface. When the interface is disconnected, like in one of our examples, then the upper bound is infinite.

* Corresponding author: e-mail: metz@math.uni-bielefeld.de, Phone: +49 521 106 5011, Fax: +49 521 106 6480
** e-mail: peter.grabner@tugraz.at, Phone: +43 316 873 7124, Fax: +43 316 873 7126

Theorem 7.3 interprets these result in terms of traces. In its proof we use graph-directed constructions to rescale a given fractal near a given interface. This indicates how one can generalize the results to connect finitely many (p.c.f. self-similar) fractals at their interface, provided their structures match nicely, like in our model cases.

The overlap of this paper with Lindstrøm's results is very small since he considers mainly nonreversible processes [20, Thm. V.6]. His only reversible case ($\alpha = \beta \equiv 1$) has no free transition constant.

The organization of the paper is as follows. In Section 2 we use graph directed methods to define the two composite fractals we will work on, the house and the thumbtack. On the house the intersection is the classical Cantor set, on the thumbtack it is the unit interval. Section 3 recalls the existence and uniqueness of self-similar sets and measures in a graph-directed construction. Section 4 associates to each finitely ramified fractal a discrete Dirichlet form. The composite part of the form is scaled by a free parameter, the transition constant η_C. This defines a renormalization map Λ_η. Section 5 sketches the one to one correspondence between irreducible Λ_η-eigenvectors and self-similar Dirichlet forms on fractals. Such eigenvectors are detected by the Short-cut Test for both examples in Section 6. Section 7 describes the effect of η_C on the thumbtack via Besov spaces.

2 The construction graphs

We consider two so called nested fractals: A variant of the Sierpinski gasket with six subtriangles, which we call "3-gasket" for short, and the Vicsek fractal in Figure 1. We want to connect the two fractals in two essentially

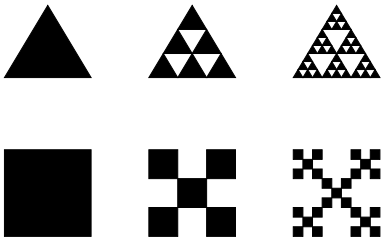

Fig. 1 The first three construction steps of the 3-gasket above and the Vicsek fractal below.

different ways: The house, that is, the lower side of the triangle intersects the top side of the square, and the thumbtack, that is, the lower side of the triangle coincides with one of the diagonals of the square. In the first case the interface is the classical middle third Cantor set and in the second it is a line segment. The difference between a totally disconnected and a connected interface will turn out to be crucial. We will consider the two composites as graph directed constructions in the sense of Mauldin and Williams [21].

As a graph directed construction the house has three "building blocks" or components, the triangle "T", the square "S" and the composite "C" in the shape of a house, as depicted in Figure 2. We need 20 contractions

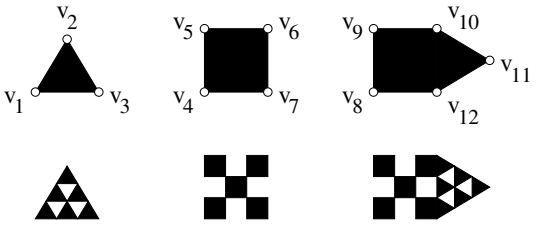

Fig. 2 The three building blocks of the house in the first line and their respective refinements in the second line

$\psi_1, \dots, \psi_{20}$ by $\frac{1}{3}$ to define the house as a graph directed construction. Set $V := \{T, S, C\}$ and $\mathbb{R}^2_v := \mathbb{R}^2 \times \{v\}$, for $v \in V$. Let us say that $\psi_1, \dots, \psi_6 : \mathbb{R}^2_T \to \mathbb{R}^2_T$ define the scaled triangles inside the triangle. The scaled squares inside the square are produced by $\psi_7, \dots, \psi_{11} : \mathbb{R}^2_S \to \mathbb{R}^2_S$. The scaled triangles inside the house are given by $\psi_{12}, \dots, \psi_{15} : \mathbb{R}^2_T \to \mathbb{R}^2_C$, the scaled squares inside the house by $\psi_{16}, \dots, \psi_{18} : \mathbb{R}^2_S \to \mathbb{R}^2_C$ and the scaled houses inside the house by $\psi_{19}, \psi_{20} : \mathbb{R}^2_C \to \mathbb{R}^2_C$. Let $e \in E := \{1, \dots, 20\}$ and consider $\psi_e : \mathbb{R}^2_w \to \mathbb{R}^2_v$. Define the domain of ψ_e by $\mathrm{dom}(e) := w$ and the target by $\mathrm{tar}(e) := v$. We think of e as

pointing from $\mathrm{tar}(e)$ to $\mathrm{dom}(e)$, the convention used by Mauldin and Williams. This defines the construction graph (V, E).

To construct the thumbtack we glue the 3-gasket to the diagonal of the Vicsek fractal in $\mathbb{R}^3$. Therefore Figure 3, the analog of Figure 2, shows only a perspective view of sketched sets. As a graph directed construction the

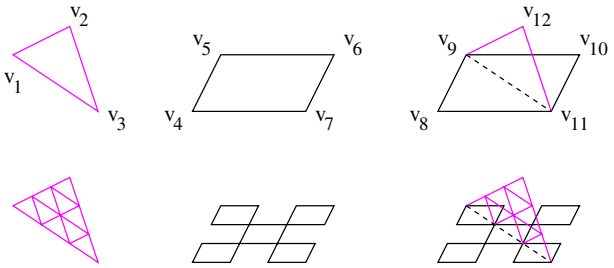

Fig. 3 (Online colour at: www.mn-journal.org) The three sketched building blocks of the thumbtack in the first line and their respective refinements in the second line. The interface is given by the dashed line.

thumbtack has three components, the triangle "T", the square "S" and the composite "C" in the shape of a thumbtack. This time we need 19 contractions $\psi_1, \ldots, \psi_{19}$ by $\frac{1}{3}$. Set $V := \{T, S, C\}$ and $\mathbb{R}^3_v := \mathbb{R}^3 \times \{v\}$, for $v \in V$. The $\psi_1, \ldots, \psi_6 : \mathbb{R}^3_T \to \mathbb{R}^3_T$ define the six scaled triangles inside the triangle, the $\psi_7 \ldots, \psi_{11} : \mathbb{R}^3_S \to \mathbb{R}^3_S$ give the five scaled squares inside the square. Finally, $\psi_{12}, \ldots, \psi_{14} : \mathbb{R}^3_T \to \mathbb{R}^3_C$ move the scaled triangles to their respective positions inside the thumbtack, $\psi_{15}, \psi_{16} : \mathbb{R}^3_S \to \mathbb{R}^3_C$ arranges the two scaled squares inside the thumbtack and $\psi_{17}, \psi_{18}, \psi_{19} : \mathbb{R}^3_C \to \mathbb{R}^3_C$ defines the scaled thumbtacks inside the thumbtack. Set $E := \{1, \ldots, 19\}$, and the construction graph is again denoted by (V, E).

3 Self-similar sets and measures

Depending on the composite under consideration let $m = 2, 3$. For $M \subset \mathbb{R}^m \times V$ define the refinement map by

$$\Psi(M) := \bigcup_{e \in E} \psi_e\big(M \cap \mathbb{R}^m_{\mathrm{dom}(e)}\big).$$

A contraction argument, like in [21, Thm. 1], proves the existence and uniqueness of nonvoid compacts $K_v \subset \mathbb{R}^m_v$, for $v \in V$, such that

$$K_v = \bigcup_{e \in E, \mathrm{tar}(e) = v} \psi_e\big(K_{\mathrm{dom}(e)}\big).$$

Thus $F := K_T \cup K_S \cup K_C$ is a fixed point of Ψ and therefore termed a self-similar set.

A subgraph of the construction graph (V, E) is termed strongly connected, when every two vertices are connected by a directed path. Hence (V, E) has three strongly connected components T, S and C. Since our construction graphs satisfy the "open set condition", [4, Thm. 6.4.8] shows that we could calculate a Hausdorff dimension for every strongly connected component via [21, Thm. 3]. Here it is simpler to use the self-similarity dimension in [6, Thm. 9.3]. This is possible because all our strongly connected components consist of a single vertex with a loop. The T-component defines the 3-gasket K_T with 6 subtriangles and Hausdorff dimension $\frac{\ln 6}{\ln 3}$. The S-component defines the Vicsek fractal K_S with Hausdorff dimension $\frac{\ln 5}{\ln 3}$. The C-component defines different sets in the house and in the thumbtack case. For the house it is the classical middle third Cantor set with Hausdorff dimension $\frac{\ln 2}{\ln 3}$. For the thumbtack it is just a line segment with Hausdorff dimension 1.

To define self-similar measures on our self-similar sets we have to choose refinement weights $p_e > 0$, for $e \in E$, such that

$$\sum_{e \in E, \mathrm{tar}(e) = v} p_e = 1 \quad (v \in V).$$

For a measure μ on the Borel sets of $\mathbb{R}^m_{\mathrm{dom}(e)}$ we define the image measure $\psi_e(\mu)(\cdot) = \mu\big(\psi_e^{-1}(\cdot)\big)$ on the Borel sets of $\mathbb{R}^m_{\mathrm{tar}(e)}$. Now the refinement map

$$\Psi(\mu) := \sum_{e\in E} p_e \cdot \psi_e(\mu)$$

defines a new measure. The above choice of refinement weights guarantees that we end up with $\Psi(\mu)(K_v) = 1$ when we started with $\mu(K_v) = 1$ for all $v \in V$. According to [5, Thm. 3.3.16] there exists a unique Borel measure ξ which is fixed by Ψ and has total mass 1 on each K_v, $v \in V$.

To guarantee that ξ restricted to K_T is the $\frac{\ln 6}{\ln 3}$-dimensional normalized Hausdorff measure on the 3-fractal, we have to choose

$$p_1 := \ldots := p_6 := \frac{1}{6}.$$

The $\frac{\ln 5}{\ln 3}$-dimensional normalized Hausdorff measure on the Vicsek fractal, K_S, is realized by the choice

$$p_7 := \ldots := p_{11} := \frac{1}{5}.$$

On the composite of the house we put equal weights on equal shapes.

$$\begin{aligned}\text{house}: \quad p_{12},\ldots,p_{15} &:= \frac{1}{4}\cdot\frac{\eta_T}{\eta_T+\eta_S+\eta_C},\\ p_{16},p_{17},p_{18} &:= \frac{1}{3}\cdot\frac{\eta_S}{\eta_T+\eta_S+\eta_C},\\ p_{19},p_{20} &:= \frac{1}{2}\cdot\frac{\eta_C}{\eta_T+\eta_S+\eta_C}.\end{aligned}$$

The exact values will be motivated in Section 5. On the interface of the thumbtack we follow the same strategy.

$$\begin{aligned}\text{thumbtack}: \quad p_{12},p_{13},p_{14} &:= \frac{1}{3}\cdot\frac{\eta_T}{\eta_T+\eta_S+\eta_C},\\ p_{15},p_{16} &:= \frac{1}{2}\cdot\frac{\eta_S}{\eta_T+\eta_S+\eta_C},\\ p_{17},p_{18},p_{19} &:= \frac{1}{3}\cdot\frac{\eta_C}{\eta_T+\eta_S+\eta_C}.\end{aligned}$$

4 The skeleton networks

Let us denote the extremal points of the initial shapes as indicated in the first line of Figure 2 or 3 by $V_0 := \{v_1,\ldots,v_{12}\}$. They are our vertices of generation 0. The n-th generation is given by $V_n := \Psi^n(V_0)$, for $n \in \mathbb{N}$.

The vertices V_0 will now be endowed with weighted edges or a so called conductance. This results in a so called electrical resistor network [3]. Consider a function $c_0 : V_0^2 \to \mathbb{R}_+$ which is symmetric, vanishes on the diagonal and assumes only the values d_1, d_2 on the triangle and the square as listed below:

$$\begin{aligned} &d_1 \quad \text{on every} \quad \{v_i,v_j\} \subset \{v_1,v_2,v_3\},\\ &d_2 \quad \text{on every} \quad \{v_i,v_j\} \subset \{v_4,\ldots,v_7\}.\end{aligned} \tag{4.1}$$

As a nested fractal the 3-gasket defines a self-similar fractal Laplacian when all its conductances are equal [8]. This is the reason for the choice of d_1. The same holds for the Vicsek fractal by [22], which justifies the choice of d_2. Further restrictions on c_0 will be imposed later. On each building block K_v we define a symmetric, discrete Dirichlet form $\mathcal{E}_0^v(\cdot,\cdot)$ in the sense of [7] via polarization and the quadratic form (energy)

$$\mathcal{E}_0^v(f) := \frac{1}{2}\sum_{x,y\in V_0\cap K_v} (f(y)-f(x))^2 c_0(x,y), \tag{4.2}$$

for $v \in V$ and $f : V_0 \to \mathbb{R}$. Then $\mathcal{E}_0 := \mathcal{E}_0^T + \mathcal{E}_0^S + \mathcal{E}_0^C$ defines a Dirichlet form on V_0.

To define the refinement map on energies we choose transition weights $\eta_e > 0$, for $e \in E$. For $f : V_1 \to \mathbb{R}$ we define a Dirichlet form on V_1 by

$$\mathcal{E}_1(f) := \Psi_\eta(\mathcal{E}_0)(f) := \sum_{e \in E} \eta_e \cdot \mathcal{E}_0^{\mathrm{dom}(e)}(f \circ \psi_e).$$

The trace of $\mathcal{E}_1$ on V_0 is given for $f : V_0 \to \mathbb{R}$ by

$$\mathrm{Tr}_{V_0}(\mathcal{E}_1)(f) := \inf\{\mathcal{E}_1(g) \mid g : V_1 \to \mathbb{R},\ g|_{V_0} = f\}.$$

By the Dirichlet principle, [16, Thm. 2.1.6], this solves the $\mathcal{E}_1$-Dirichlet problem on the "open" set $V_1 \setminus V_0$ with data f on the "boundary" V_0. Finally, the renormalization map is defined to be

$$\Lambda_\eta := \mathrm{Tr}_{V_0} \circ \Psi_\eta.$$

In physics the action of Λ_η is called "coarse graining renormalization" [11]. It can be calculated by Theorem 4.1. Every $\mathcal{E}_0 \in \mathbb{D}$ defines a graph $\Gamma(\mathcal{E}_0)$ with vertex set V_0 and edge set $\{\{x, y\} \subset V_0 \mid c_{\mathcal{E}_0}(x, y) > 0\}$. In the same way $\mathcal{E}_1$ defines a graph $\Gamma(\mathcal{E}_1)$ with vertex set V_1 and analogous edge set. We call a Dirichlet form irreducible, when its graph is connected.

Theorem 4.1 (Schur complement formula [1, Eq. 6, Thm. 6]) *Let $W \neq \emptyset$ be a finite set and c a conductance on W whose Dirichlet form $\mathcal{A}$, defined by* (4.2)*, is irreducible. Consider the Dirichlet operator A of $\mathcal{A}$ as a matrix with respect to the standard orthonormal basis of $\mathbb{R}^W$. Choose $\emptyset \neq I \subset W$ and define $B := W \setminus I$. Let A_{ST} be the submatrix of A with rows from S and columns from T, for $S, T \in \{B, I\}$. Denote the matrix of the Dirichlet operator of* $\mathrm{Tr}_B(\mathcal{A})$ *by* $\mathrm{Tr}_B(A)$*. Then* $\mathrm{Tr}_B(A) = A_{BB} - A_{BI}(A_{II})^{-1}A_{IB}$.

The above Schur complement formula can be used to prove the well-known equations for the effective resistance of resistors in line and in parallel. It allows us to remove dangling ends from resistor networks and it shows that $\mathrm{Tr}_B \circ \mathrm{Tr}_C = \mathrm{Tr}_B$ for $B \subset C \subset W$.

We want to decide for which transition weights $\eta := (\eta_T, \eta_S, \eta_C)$ there exists a unique (up to positive multiples) solution of

$$\Lambda_\eta(\mathcal{E}) = \gamma\mathcal{E} \quad (\gamma \in \mathbb{R}, \mathcal{E} \in \mathbb{D}^\circ). \tag{4.3}$$

Such an eigenvector defines a "Laplacian" on F as we will see in Section 5. Again the triangle, the square and the composite define irreducible subproblems. When we evaluate Λ_η only on conductances between points of the triangle, $\{v_1, v_2, v_3\}$, then

$$\eta_T = \frac{15}{7}$$

is the only transition weight guaranteeing a Λ_η-fixed point [8]. Doing the same on the square, $\{v_4, \ldots, v_7\}$, we find the only possible transition weight

$$\eta_S = 3$$

according to [22]. Therefore let us fix η_T and η_S to the above values. This leaves only η_C as a free variable in (4.3).

On the house we want c_0 to be invariant under the reflection in the line through v_{11} and $\frac{v_8+v_9}{2}$. This requires the following choice:

$$\begin{array}{lllll} \text{house}: & d_3 & \text{for} & \{v_8, v_{12}\}, \{v_9, v_{10}\}, \\ & d_4 & \text{for} & \{v_{10}, v_{11}\}, \{v_{11}, v_{12}\}, \\ & d_5 & \text{for} & \{v_8, v_{11}\}, \{v_9, v_{11}\}, \\ & d_6 & \text{for} & \{v_8, v_{10}\}, \{v_9, v_{12}\}, \\ & d_7 & \text{for} & \{v_{10}, v_{12}\}, \\ & d_8 & \text{for} & \{v_8, v_9\}. \end{array} \tag{4.4}$$

On the thumbtack we want c_0 to be invariant under the reflections in two planes, one spanned by $\{v_9, v_{11}, v_{12}\}$ and one spanned by $\{v_8, v_{10}, v_{12}\}$. This requires the choice:

$$\begin{array}{lllll} \text{thumbtack}: & d_3 & \text{for} & \{v_8,v_9\},\{v_9,v_{10}\},\{v_{10},v_{11}\},\{v_8,v_{11}\}, \\ & d_4 & \text{for} & \{v_9,v_{12}\},\{v_{11},v_{12}\}, \\ & d_5 & \text{for} & \{v_8,v_{12}\},\{v_{10},v_{12}\}, \\ & d_6 & \text{for} & \{v_8,v_{10}\}, \\ & d_7 & \text{for} & \{v_9,v_{11}\}. \end{array} \tag{4.5}$$

5 Dirichlet forms on fractals

The construction of an irreducible, regular, local, conservative and symmetric Dirichlet form on our fractal follows [10, Sect. 4], which is itself an adaption of the arguments in [16, Sect. 3], where single component fractals are treated.

Suppose we have found a unique solution $\mathcal{F}$ of (4.3) for some $\eta_C > 0$. Define

$$\mathcal{F}_n := \Psi_\eta^n(\mathcal{F}) \quad (n \in \mathbb{N}).$$

When $\eta_v > 1$, for $v \in V$, this defines a so called regular harmonic structure for which our constructions work. By definition $\eta_T, \eta_S > 1$. So we have to require

$$\eta_C > 1. \tag{5.1}$$

Set $V_\infty := \bigcup_{n\in\mathbb{N}} V_n$ and let $m = 2, 3$ depend on the composite in question. Since $\mathcal{F}$ is a fixed point, we have

$$\mathcal{F}_n(f|_{V_n}) \le \mathcal{F}_{n+1}(f|_{V_{n+1}}) \quad (f : V_\infty \to \mathbb{R}, n \in \mathbb{N}).$$

By [10, Lemma 4.7] every $f : V_\infty \to \mathbb{R}$, for which $(\mathcal{F}_n(f|_{V_n}))_n$ is bounded from above, is uniformly continuous on $V_\infty \subset \mathbb{R}^m \times V$. So it can be extended to a continuous function $f \in C(F, \mathbb{R})$. This enables us to define the quadratic form $\mathcal{E} : \mathcal{D}(\mathcal{E}) \to \mathbb{R}_+$ given by

$$\begin{aligned} \mathcal{D}(\mathcal{E}) &:= \left\{ f \in C(F,\mathbb{R}) \mid \sup_n \mathcal{F}_n(f|_{V_n}) < \infty \right\}, \\ \mathcal{E}(f) &:= \sup_n \mathcal{F}_n(f|_{V_n}) = \lim_{n\to\infty} \mathcal{F}_n(f|_{V_n}). \end{aligned}$$

It defines via polarization a Dirichlet form of the desired type on $L^2(F, \xi)$ [10, Thm. 4.9]. Here ξ is the self-similar measure of Section 3, depending on the house or the thumbtack setup. The refinement weights of ξ have been chosen in Section 3 in such a way that ξ turns out to be an invariant measure of the stochastic process defined by $(\mathcal{E}, \mathcal{D}(\mathcal{E}))$ on F [7, Chap. 4]. The invariant measure is not unique because the process lives on three different connected components. We have chosen the version with total mass 1 on each component.

6 The Short-cut Test

The fixed point problem (4.3) can be treated by the Short-cut Test in [23]. To this end we have to define the domain of Λ_η. Let $\mathbb{D}$ be the set of all Dirichlet forms given in (4.2) by the conductances in (4.1) and those in (4.4) or (4.5), respectively. These conductances take on the values $d_1, \dots, d_k$, where $k = 8$ for the house and $k = 7$ for the thumbtack. Together with $c_\mathcal{E}(x, y) = -\mathcal{E}\big(1_{\{x\}}, 1_{\{y\}}\big)$, for $x \ne y \in V_0$, and the fact that all our forms vanish on constants, this defines a linear isomorphism $T : \mathbb{D} - \mathbb{D} \to \mathbb{R}^k$. For $\mathcal{E} \in \mathbb{D} - \mathbb{D}$ let us denote the i-th component of $T(\mathcal{E})$ by $d_i(\mathcal{E})$, because for $\mathcal{E} \in \mathbb{D}$ it is the conductance d_i. Evaluating $\mathcal{E} \in \mathbb{D}$ only on functions which vanish on $V_0 \setminus \{v_1, v_2, v_3\}$ and taking our choice of η_T into account, or evaluating only at functions vanishing on $V_0 \setminus \{v_4, \dots, v_7\}$ and taking our choice of η_S into consideration, we derive

$$d_i(\Lambda_\eta(\mathcal{E})) = d_i(\mathcal{E}) \quad (i = 1, 2;\ \mathcal{E} \in \mathbb{D}). \tag{6.1}$$

When $\mathcal{E} \in \mathbb{D} \setminus \{0\}$, then it defines a $\mathbb{D}$-part

$$\mathbb{D}_{\mathcal{E}} := \{\mathcal{A} \in \mathbb{D} \,|\, \Gamma(\mathcal{A}) = \Gamma(\mathcal{E})\}.$$

Because of the following lemma, Λ_η acts on the set of $\mathbb{D}$-parts supplemented by $\{0\}$.

Lemma 6.1 ([23, Lemma 16]) *For $\mathcal{E} \in \mathbb{D}$ and different $x, y \in V_0$, $c_{\Lambda_\eta(\mathcal{E})}(x, y) > 0$ if and only if there exists a path in $\Gamma(\mathcal{E}_1)$ connecting x to y and avoiding $V_0 \setminus \{x, y\}$.*

So a $\mathbb{D}$-part containing a Λ_η-fixed point must be Λ_η-invariant. The latter can be detected graphically via Lemma 6.1. Furthermore, $\Gamma(\mathcal{A}) \subset \Gamma(\mathcal{E})$ implies $\Gamma(\Lambda_\eta(\mathcal{A})) \subset \Gamma(\Lambda_\eta(\mathcal{E}))$. Therefore we write $\mathbb{D}_1 \leq \mathbb{D}_2$ for $\mathbb{D}$-parts $\mathbb{D}_1, \mathbb{D}_2$ with $\Gamma(\mathbb{D}_1) \subseteq \Gamma(\mathbb{D}_2)$.

For $\mathcal{E} \in \mathbb{D}$ define $\ker \mathcal{E} := \{f : V_0 \to \mathbb{R} \,|\, \mathcal{E}(f) = 0\}$. The minimum principle, [16, Prop. 2.1.7], shows that $\ker \mathcal{E}$ is the set of functions which are constant on the connected components of $\Gamma(\mathcal{E})$. Suppose we have found a reducible Λ_η-fixed point $\mathcal{F} \in \mathbb{D}$. Then $\mathbb{D}_{\mathcal{F}}$ is Λ_η-invariant by Lemma 6.1. To perform the Short-cut Test we will have to calculate eigenvalues of $\Lambda_\eta(\infty\mathcal{F} + \cdot)$. The Λ_η-invariance of $\mathbb{D}_{\mathcal{F}}$ implies for $\mathcal{E} \in \mathbb{D}$ that $\Lambda_\eta(\infty\mathcal{F} + \mathcal{E})(f) < \infty$ if and only if $f \in \ker \mathcal{F}$. So we only have to evaluate at functions which are constant on the connected components of $\Gamma(\mathcal{F})$.

Remark 6.2 The eigenvalues of $\Lambda_\eta(\infty\mathcal{F} + \cdot)$ can be found as follows: Identify each connected component of $\Gamma(\mathcal{F})$ with a single new point. The conductances on edges between new points are the sum of the conductances between the corresponding components [23, Lemma 17]. The same happens for $\Gamma(\mathcal{F}_1)$. So we are back to new and simpler Dirichlet forms with finite conductances on which Λ_η also acts because of the Λ_η-invariance of $\mathbb{D}_{\mathcal{F}}$.

By Remark 6.2 it is clear that any two Λ_η-invariant forms $\mathcal{E}, \mathcal{F} \in \mathbb{D}$ with $\ker \mathcal{E} = \ker \mathcal{F}$ result in the same eigenvalue problem because their graphs have the same set of connected components. So we only have to apply the remark to $\mathbb{D}$-parts with different kernels. To illustrate the shorting effect of the remark let us consider the composite of the house as depicted in Figure 5. We set $d_1 := d_2 := \infty$ and apply the remark. The result is shown in Figure 4. All the sums in the figure come from the reduction of multiple edges to simple edges. The reader might wonder, where the second edge with conductance d_4 went. It became a loop at vertex v_{11}. They do not contribute to the energy by (4.2), so we erased the d_4-loops.

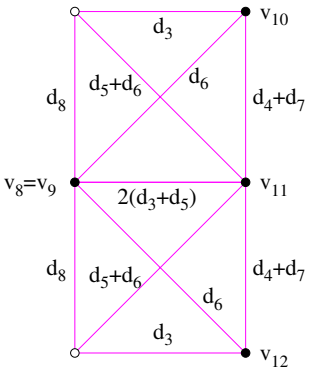

Fig. 4 (Online colour at: www.mn-journal.org) The short circuited composite of the house ($d_1 = d_2 = \infty$)

Suppose all Λ_η-invariant $\mathbb{D}$-parts have different kernels. Let $\mathbb{D}_1$ be a $\mathbb{D}$-part containing a Λ_η-fixed point $\mathcal{F}$. Let $\mathbb{D}_2$ be a Λ_η-invariant $\mathbb{D}$-part strictly bigger than $\mathbb{D}_1$. We say that $\mathbb{D}_1$ is *weakly repellent* in $\overline{\mathbb{D}_2}$ (the set of all $\mathbb{D}$-parts with kernels at least as big as $\ker \mathbb{D}_2$), when the map $\Lambda_\eta(\infty\mathcal{F} + \cdot)$ has an eigenvector in $\overline{\mathbb{D}_2}$ whose eigenvalue γ is strictly bigger than the eigenvalue of $\mathbb{D}_1$. Here comes the Short-cut Test.

Theorem 6.3 ([23, Thm. 26]) *Suppose all Λ_η-invariant $\mathbb{D}$-parts have different kernels and every $\mathbb{D}$-part containing a Λ_η-fixed point $\mathcal{F}$ is weakly repellent in $\mathbb{D}$. Then there exists a unique irreducible Λ_η-fixed point in $\mathbb{D}$.*

We can verify the assumptions of Theorem 6.3 step by step.

Lemma 6.4 ([23, Prop. 9 (i), Rem. 31]) *Suppose all Λ_η-invariant $\mathbb{D}$-parts have different kernels. Assume the $\mathbb{D}$-part $\mathbb{D}_1$ contains a Λ_η-eigenvector with eigenvalue λ_1 and there exists a $\mathbb{D}$-part $\mathbb{D}_2$ such that $\mathbb{D}_1 \leq \mathbb{D}_2$ and* $\ker \mathbb{D}_1 \neq \ker \mathbb{D}_2$.

(a) *When $\mathbb{D}_2$ contains a Λ_η-eigenvector with eigenvalue λ_2, then $\lambda_1 \leq \lambda_2$.*

(b) *When $\mathbb{D}_1$ is weakly repellent in $\overline{\mathbb{D}_2}$, then $\mathbb{D}_1$ is weakly repellent in $\mathbb{D}$.*

6.1 The house

Employing Lemma 6.1 we can find the Λ_η-invariant $\mathbb{D}$-parts graphically in Figure 5. Every $\mathbb{D}$-part is characterized by a unique set of positive conductances. Thus we index our $\mathbb{D}$-part by representative conductances $(d_1, \ldots, d_8) \in \{0,1\}^8$, with $d_1 = d_2$ because of (6.1). We find the Λ_η-invariant $\mathbb{D}$-parts $\mathbb{D}_3, \mathbb{D}_4, \mathbb{D}_5$ and $\mathbb{D}^\circ$ below. They all connect the triangle, $\{v_1, v_2, v_3\}$, and the square, $\{v_4, \ldots, v_7\}$. The remaining connected components are:

$$\begin{aligned}
\mathbb{D}_3 := \mathbb{D}_{(1,1,0,0,0,0,0,1)} &: \{v_8, v_9\}, \{v_{10}\}, \{v_{11}\}, \{v_{12}\},\\
\mathbb{D}_4 := \mathbb{D}_{(1,1,0,0,1,0,0,1)} &: \{v_8, v_9, v_{11}\}, \{v_{10}\}, \{v_{12}\},\\
\mathbb{D}_5 := \mathbb{D}_{(1,1,0,1,0,0,1,1)} &: \{v_8, v_9\}, \{v_{10}, v_{11}, v_{12}\},\\
\mathbb{D}^\circ = \mathbb{D}_{(1,1,1,1,1,1,1,1)} &: \{v_8, \ldots, v_{12}\}.
\end{aligned}$$

So all invariant $\mathbb{D}$-parts have different kernels.

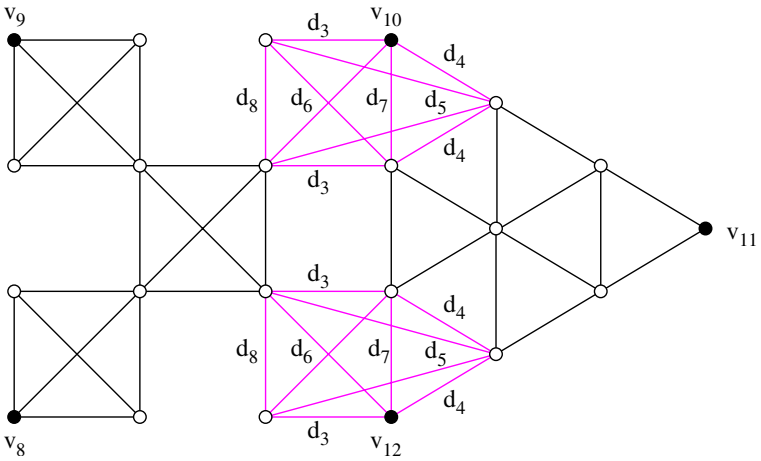

Fig. 5 (Online colour at: www.mn-journal.org) The refinement of the composite of the house

Every element $\mathcal{E}$ of a Λ_η-invariant $\mathbb{D}$-part satisfies $d_1(\mathcal{E}), d_2(\mathcal{E}) > 0$. So every Λ_η-eigenvector they contain must be a Λ_η-fixed point by (6.1) or there is no eigenvector at all. In the latter case we need not employ Theorem 6.3. Nevertheless, we will check its eigenvalue inequality to save the work of detecting fixed points. Denote the possible Λ_η-eigenvalue in $\mathbb{D}_i$ by λ_i and an eigenvalue of the short circuited model by γ_i for $i = 3, 4, 5$.

setup	d_1	d_2	d_3	d_4	d_5	d_6	d_7	d_8	λ_i	γ_i
$\mathbb{D}_3 \subset \overline{\mathbb{D}_4}$	∞	∞	0	0	d_5	0	0	∞	1	$2\eta_C$
$\mathbb{D}_4 \subset \mathbb{D}$	∞	∞	d_3	d_4	∞	d_6	d_7	∞	1	η_C
$\mathbb{D}_5 \subset \mathbb{D}$	∞	∞	d_3	∞	d_5	d_6	∞	∞	1	$2\eta_C$

Table 1 The chain $\mathbb{D}_3 \leq \mathbb{D}_4 \leq \mathbb{D}^\circ$

We will apply Lemma 6.4 to the chain $\mathbb{D}_3 \leq \mathbb{D}_4 \leq \mathbb{D}^\circ$ and Theorem 6.3 to $\mathbb{D}_5 \leq \mathbb{D}^\circ$. The eigenvalue inequalities $\gamma_i > \lambda_i$, for $i = 3, 4, 5$, are obviously satisfied under the condition

$$\eta_C > 1. \tag{6.2}$$

When we apply Lemma 6.4 and Theorem 6.3 as mentioned above, then the weak repellence of $\mathbb{D}_2, \mathbb{D}_3$ and $\mathbb{D}_4$ follows and a last application of Theorem 6.3 yields a unique irreducible fixed point in $\mathbb{D}$. Since $\mathbb{D}^\circ$ is the only Λ_η-invariant $\mathbb{D}$-part consisting of irreducible forms, the fixed point must even lie in $\mathbb{D}^\circ$, that is, all its conductances are strictly positive.

Theorem 6.5 *For $\eta_C > 1$ there exists a unique (up to positive multiples) Λ_η-fixed point with strictly positive and finite conductances on the house.*

6.2 The thumbtack

Because of (6.1) we also restrict ourselves to $d_1 = d_2$. Again we have to find the Λ_η-invariant $\mathbb{D}$-parts graphically in Figure 6 by Lemma 6.1. We find the Λ_η-invariant $\mathbb{D}$-part $\mathbb{D}_1 := \mathbb{D}_{(0,0,0,0,0,0,1)}$, $\mathbb{D}_2, \ldots, \mathbb{D}_{10}$ below and $\mathbb{D}^\circ$.

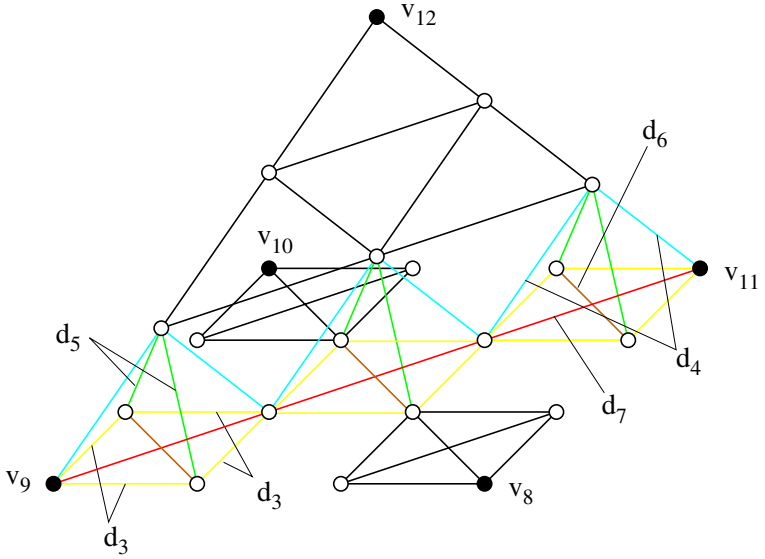

Fig. 6 (Online colour at: www.mn-journal.org) The refinement of the composite of the thumbtack. The lines with conductance d_3 are not visible on the black and white print out

In $\mathbb{D}_1$ all vertices of V_0 are isolated except $\{v_9, v_{11}\}$. All other invariant $\mathbb{D}$-parts connect the triangle, $\{v_1, v_2, v_3\}$, and the square, $\{v_4, v_5, v_6, v_7\}$. The remaining connected components are

$$
\begin{aligned}
\mathbb{D}_2 := \mathbb{D}_{(1,1,0,0,0,0,0)} &: \{v_8\}, \{v_9\}, \{v_{10}\}, \{v_{11}\}, \{v_{12}\},\\
\mathbb{D}_3 := \mathbb{D}_{(1,1,0,0,0,0,1)} &: \{v_8\}, \{v_9, v_{11}\}, \{v_{10}\}, \{v_{12}\},\\
\mathbb{D}_4 := \mathbb{D}_{(1,1,0,0,0,1,0)} &: \{v_8, v_{10}\}, \{v_9\}, \{v_{11}\}, \{v_{12}\},\\
\mathbb{D}_5 := \mathbb{D}_{(1,1,0,0,0,1,1)} &: \{v_8, v_{10}\}, \{v_9, v_{11}\}, \{v_{12}\},\\
\mathbb{D}_6 := \mathbb{D}_{(1,1,1,0,0,1,1)} &: \{v_8, \ldots, v_{11}\}, \{v_{12}\}\\
\mathbb{D}_7 := \mathbb{D}_{(1,1,0,0,1,1,0)} &: \{v_8, v_{10}, v_{12}\}, \{v_9\}, \{v_{11}\},\\
\mathbb{D}_8 := \mathbb{D}_{(1,1,0,0,1,1,1)} &: \{v_8, v_{10}, v_{12}\}, \{v_9, v_{11}\}\\
\mathbb{D}_9 := \mathbb{D}_{(1,1,0,1,0,0,1)} &: \{v_8\}, \{v_9, v_{11}, v_{12}\}, \{v_{10}\},\\
\mathbb{D}_{10} := \mathbb{D}_{(1,1,0,1,0,1,1)} &: \{v_8, v_{10}\}, \{v_9, v_{11}, v_{12}\}\\
\mathbb{D}^\circ := \mathbb{D}_{(1,1,1,1,1,1,1)} &: \{v_8, \ldots, v_{12}\}.
\end{aligned}
$$

All invariant $\mathbb{D}$-parts have different kernels.

The Λ_η-eigenvalues of $\mathbb{D}_1$: Choose an $\mathcal{E} \in \mathbb{D}$ with a single positive conductance d_7. Then Theorem 4.1, or more precisely the rule for resistors in series, shows that $d_7(\Lambda_\eta(\mathcal{E})) = (\eta_C d_7)/3$. Hence $\mathbb{D}_1$ contains an eigenvector $\mathcal{F}^{(1)}$ with eigenvalue $\eta_C/3$. According to $\mathbb{D}_1 \leq \mathbb{D}^\circ$ and Lemma 6.4 all eigenvalues of $\mathbb{D}^\circ$ are not less than any eigenvalue of $\mathbb{D}_1$. Thus we have to require $\eta_C \leq 3$ in order to avoid a contradiction to the existence

of fixed points in $\mathbb{D}^\circ$. Together with (5.1) we arrive at

$$1 < \eta_C \leq 3. \tag{6.3}$$

Again every $\mathbb{D}$-part, except $\mathbb{D}_1$, contains a Λ_η-fixed point or no Λ_η-eigenvector at all by (6.1). In the latter case we need not employ Theorem 6.3. But we will check the eigenvalue inequality of this theorem for all Λ_η-invariant $\mathbb{D}$-parts in order to save the work of detecting fixed points. Denote the possible Λ_η-eigenvalue in $\mathbb{D}_i$ by λ_i and an eigenvalue of the short circuited model by γ_i, for $1 \leq i \leq 10$.

setup	d_1	d_2	d_3	d_4	d_5	d_6	d_7	λ_i	γ_i
$\mathbb{D}_2 \subset \overline{\mathbb{D}_4}$	∞	∞	0	0	0	d_6	0	1	η_C
$\mathbb{D}_4 \subset \overline{\mathbb{D}_7}$	∞	∞	0	0	d_5	∞	0	1	$2\eta_C$
$\mathbb{D}_7 \subset \mathbb{D}$	∞	∞	d_3	d_4	∞	∞	$d_7 := 0$	1	$\geq \eta_C$

Table 2 The chain $\mathbb{D}_2 \leq \mathbb{D}_4 \leq \mathbb{D}_7 \leq \mathbb{D}^\circ$

Our next task is to check the eigenvalue inequality of "weak repellence" for several chains. The first one is $\mathbb{D}_2 \leq \mathbb{D}_4 \leq \mathbb{D}_7 \leq \mathbb{D}^\circ$. The meaning of "$d_7 := 0$" in the last row is that we define d_7 to vanish and calculate an eigenvalue η_C of the short circuited model. Thus $\gamma_i \geq \eta_C$ by Lemma 6.4(a). In total we see that $\gamma_i > \lambda_i$, for $i = 2, 4, 7$, is valid under the condition (6.3). Lemma 6.4 applied to $\mathbb{D}_2 \leq \mathbb{D}_4 \leq \mathbb{D}_7 \leq \mathbb{D}^\circ$ now implies that $\mathbb{D}_2$, $\mathbb{D}_4$ and $\mathbb{D}_7$ are weakly repellent in $\mathbb{D}$ under the condition (6.3).

setup	d_1	d_2	d_3	d_4	d_5	d_6	d_7	λ_i	γ_i
$\mathbb{D}_3 \subset \overline{\mathbb{D}_9}$	∞	∞	0	d_4	0	0	∞	1	$6\eta_C$
$\mathbb{D}_2 \subset \overline{\mathbb{D}_9}$	∞	∞	0	d_4	0	0	$d_7 := 0$	1	$\geq \eta_C$
$\mathbb{D}_9 \subset \mathbb{D}$	∞	∞	d_3	∞	d_5	d_6	∞	1	$\geq \eta_C$

Table 3 The chains $\mathbb{D}_2, \mathbb{D}_3 \leq \mathbb{D}_9 \leq \mathbb{D}^\circ$

Next we use the three chains $\mathbb{D}_1, \mathbb{D}_2, \mathbb{D}_3 \leq \mathbb{D}_9 \leq \mathbb{D}^\circ$. Weak repellence of $\mathbb{D}_1 \subset \overline{\mathbb{D}_9}$: We note that $\lambda_1 = \eta_C/3$. Consider $\mathcal{E} \in \mathbb{D}$ with the conductances $(d_1, d_1, 0, d_4, 0, 0, \infty)$ and $d_1, d_4 > 0$. Because of (6.1) it suffices to look at the composite. Here only one edge remains. The action of $\Lambda_\eta(\infty\mathcal{F}^{(1)} + \cdot)$ on its conductance is

$$2d_4 \longmapsto \frac{10\eta_C d_4(28\eta_C d_4 + 135)}{98\eta_C^2 d_4^2 + 525\eta_C d_4 + 225}.$$

So the eigenvalue of $\Lambda_\eta\big(\infty\mathcal{F}^{(x)} + \mathcal{E}\big)$ is strictly bigger than $\eta_C/3$ if and only if $98\eta_C^2 d_4^2 + 105\eta_C d_4 - 1800 < 0$. For $\eta_C d_4$ positive but near 0 the inequality holds. So we end up with (6.3). In the last row of Table 6.2 we did not calculate the conductance of the short circuited model on V_1 exactly but estimated it from below. So we got a lower estimate on γ_i. Again $\gamma_i > \lambda_i$ for $i = 2, 3, 9$ under the condition (6.3). Lemma 6.4 applied to $\mathbb{D}_1, \mathbb{D}_2, \mathbb{D}_3 \leq \mathbb{D}_9 \leq \mathbb{D}^\circ$ now implies that $\mathbb{D}_1, \mathbb{D}_2$ and $\mathbb{D}_3$ are also weakly repellent in $\mathbb{D}$ under the condition (6.3).

setup	d_1	d_2	d_3	d_4	d_5	d_6	d_7	λ_i	γ_i
$\mathbb{D}_5 \subset \overline{\mathbb{D}_8}$	∞	∞	0	0	d_5	∞	∞	1	η_C
$\mathbb{D}_8 \subset \mathbb{D}$	∞	∞	d_3	d_4	∞	∞	∞	1	$3\eta_C$

Table 4 The chain $\mathbb{D}_5 \leq \mathbb{D}_8 \leq \mathbb{D}^\circ$

The next chain is $\mathbb{D}_5 \leq \mathbb{D}_8 \leq \mathbb{D}^\circ$. Once more $\gamma_i > \lambda_i$ holds under condition (6.3). Lemma 6.4 applied to $\mathbb{D}_5 \leq \mathbb{D}_8 \leq \mathbb{D}^\circ$ shows that $\mathbb{D}_5$ and $\mathbb{D}_8$ are weakly repellent in $\mathbb{D}$ for (6.3).

setup	d_1	d_2	d_3	d_4	d_5	d_6	d_7	λ_i	γ_i
$\mathbb{D}_6 \subset \mathbb{D}$	∞	∞	∞	d_4	d_5	∞	∞	1	$3\eta_C$
$\mathbb{D}_{10} \subset \mathbb{D}$	∞	∞	d_3	∞	d_5	∞	∞	1	$\geq \eta_C$

Table 5 The chains $\mathbb{D}_6, \mathbb{D}_{10} \leq \mathbb{D}^\circ$

It remains to look at $\mathbb{D}_6, \mathbb{D}_{10} \leq \mathbb{D}^\circ$. In the last row we estimated the conductance of the short circuited model on V_1 again from below. Condition (6.3) implies $\gamma_i > \lambda_i$ for $i = 6, 10$. Lemma 6.4 applied to $\mathbb{D}_6 \leq \mathbb{D}^\circ$ and $\mathbb{D}_{10} \leq \mathbb{D}^\circ$ implies the desired weak repellence.

Another application of Theorem 6.3 now yields the existence and uniqueness of an irreducible fixed point in $\mathbb{D}$. Since $\mathbb{D}^\circ$ is the only invariant $\mathbb{D}$-part consisting of irreducible forms, we even get existence and uniqueness in $\mathbb{D}^\circ$.

Theorem 6.6 *For $1 < \eta_I \leq 3$ there exists a unique (up to positive multiples) Λ_η-fixed point with strictly positive and finite conductances on the thumbtack.*

7 Effects on and near the interface

We discuss the effects of a varying η_C on the composite fractal and on the interface between the two component fractals. Our first case is the thumbtack because it exhibits a richer structure than the house.

When $\eta_C > 3$, then d_7, the conductance along the interface, is no more finite (short circuited). To see this consider the overlap of the two component fractals. It is a line segment. We view it as being composed of three subintervals of equal size, since our contractions all have the contraction factor $\frac{1}{3}$. Thus its energy scaling, according to the rules for resistors in series, must be $\frac{1}{3}$. Since η_C^{-1} is strictly less than that, the conductance becomes infinite in the limit.

When $\eta_C = 3$, then the Vicsek set is unperturbed. Only the 3-gasket is gradually changed near the interface. The (isolated) interface has positive and finite conductance, because it has exactly the energy scaling of a line.

When $15/7 < \eta_C < 3$, then the Vicsek set and the 3-gasket are changed gradually near the interface. This is probably the most realistic setting. The exact value of η_C has to be motivated extrinsically. The isolated interface has conductance zero, because its energy scaling is strictly less than the one of a line. But there is still transport across it, as we can see from the fact that the fixed point has strictly positive conductances only.

When $\eta_C = 15/7$, then the 3-gasket is unperturbed but the Vicsek set is changed.

When $1 < \eta_C < 15/7$, then both fractals are perturbed near the interface. The conductance across the interface is lower than in the $15/7 \leq \eta_C \leq 3$ cases. Physically, this could be interpreted as the presence of a third material at the interface, for instance an alloy of the two materials.

On the house we see similar effects as on the thumbtack. But there is no short circuiting effect, because the interface is a totally disconnected Cantor set.

7.1 Interpretation via traces

In this subsection we consider exclusively the thumbtack. The techniques we use to prove the desired trace results can be generalized to the connection of finitely many (p.c.f. self-similar) fractals which intersect each other in a self-similar interface I. The idea is to redefine the given fractal K_T as a graph-directed construction which allows us to scale different copies differently. The relation between fractals and (traces of) function spaces can be found in [14] and [25]. The operators considered in the latter book are different from the Dirichlet operators of the Dirichlet form $\mathcal{E}$ considered here. We fix $\eta_C \in (1, 3)$ in accordance with Theorem 6.6. Since the thumbtack is finitely ramified, its Dirichlet form $(\mathcal{E}, \mathcal{D}(\mathcal{E}))$ induced by η_C, and killed in at least one point of V_0 in every connected component, has finite "Green's functions" [16, Thm. 3.5.7]. Hence all open sets are regular [2, Prop. VII.3.1]. Thus we can choose an open set $U \subset F$ and define the trace of $\mathcal{E}$ on U by

$$\mathrm{Tr}_U(\mathcal{E})(f) := \mathcal{E}\big(H_U^{\mathcal{E}} f\big),$$

where $f \in \mathcal{D}(\mathcal{E})$ and $H_U^{\mathcal{E}} f : F \to \mathbb{R}$ is the $\mathcal{E}$-harmonic extension of f to F, that is, it is continuous on $\overline{U}$ and $\mathcal{E}$-harmonic on U. We have a copy $K_\sharp$ of K_T in K_C and its trace

$$\mathcal{E}^\sharp := \mathrm{Tr}_{F\setminus K_\sharp}(\mathcal{E}).$$

Denote the line segment from v_9 to v_{11} by I. We will calculate the trace of the domain $\mathcal{D}(\mathcal{E}^\sharp)$ of $\mathcal{E}^\sharp$ on I for all η_C. Setting $\eta_C = \frac{15}{7}$ we recover the trace on I of the domain $\mathcal{D}(\mathcal{E}^{(T)})$ of the (self-similar) Dirichlet form $\mathcal{E}^{(T)}$ of the classical 3-gasket K_T.

In [12] Jonsson identified the domain of the (self-similar) Dirichlet form on the Sierpinski gasket as a certain Lipschitz space. His results were generalized to nested fractals in [24]. This gives us

$$\mathcal{D}(\mathcal{E}^{(T)}) = \mathrm{Lip}\left(\tfrac{\ln(90)-\ln 7}{\ln 9}, 2, \infty; K_T\right).$$

In [13] the trace on I of the domain of the Dirichlet form on the Sierpinski gasket turned out to be the Besov space $B_\alpha^{2,2}(I)$, where $\alpha = \frac{\ln 5}{\ln 4} - \frac{\ln 3/\ln 2 - 1}{2}$. This trace is analogous to classical results, that is, the drop in "differentiability" is $(d-1)/2$, where d denotes the Hausdorff dimension of the Sierpinski gasket and 1 is the dimension of I. We will slightly generalize the arguments in [13] to achieve trace results for $\mathcal{D}(\mathcal{E}^\sharp)$. In analogy with Jonsson's results on the Sierpinski gasket the trace of $\mathcal{D}\big(\mathcal{E}^{(T)}\big)$ on I should be $B_\alpha^{2,2}(I)$ for

$$\alpha = \frac{\ln(90)-\ln 7}{\ln 9} - \frac{\ln 6 - \ln 3}{\ln 9} = \frac{\ln(45)-\ln 7}{\ln 9}.$$

Theorem 7.3 for $\eta_C = \frac{15}{7}$ will verify this guess.

To indicate how the local rescaling near I of a given fractal K_T can be done in general we redefine $K_\sharp$ as a graph directed fractal: We start with two triangles, one which is used to reconstruct K_T and one on which we reconstruct $K_\sharp$. Set $V := \{T, \sharp\}$. Let $\psi_1, \ldots, \psi_6 : \mathbb{R}_T^2 \to \mathbb{R}_T^2$ define six scaled (by $\frac{1}{3}$) copies of the T-triangle inside the T-triangle. Use $\psi_7, \psi_8, \psi_9 : \mathbb{R}_T^2 \to \mathbb{R}_\sharp^2$ to define three scaled copies of the T-triangle in the upper three positions of the $\sharp$-triangle. Finally, $\psi_{10}, \psi_{11}, \psi_{12} : \mathbb{R}_\sharp^2 \to \mathbb{R}_\sharp^2$ produce three scaled copies of the $\sharp$-triangle on the three lower positions of the $\sharp$-triangle. Choose the transition weights

$$\begin{aligned}\eta_1 &:= \ldots := \eta_9 := \frac{15}{7},\\ \eta_{10} &:= \eta_{11} := \eta_{12} := \eta_C.\end{aligned}$$

When $\eta_C \neq \frac{15}{7}$, then we have broken the symmetries of the $\sharp$-triangle. Only the reflection in the line through v_{12} and $(v_9 + v_{11})/2$ leaves the transition weights of the $\sharp$-triangle invariant. Thus this triangle has two different conductances, s on the two sides of v_{12} and b on the base line from v_9 to v_{11}. We endow the T-triangle with conductance 1 on all edges. Now we can apply the new $\Lambda_\eta^\sharp$ to these conductances.

Lemma 7.1 *There exist $0 < s, b < \infty$ which are fixed under the above $\Lambda_\eta^\sharp$.*

Proof. According to Theorem 6.6 there exists a fixed point of the old Λ_η of the thumbtack. Take the trace of this fixed point on $\{v_9, v_{11}, v_{12}\}$ to find s and b. □

Let $(\mathcal{F}_n^\sharp)_n$ be the sequence of discrete Dirichlet forms defined by the corresponding $\Psi_\eta^\sharp$ on the T- and $\sharp$-triangles. Like in Section 5 this sequence determines a self-similar Dirichlet form $(\mathcal{E}^\sharp, \mathcal{D}(\mathcal{E}^\sharp))$. Let $f \in \mathcal{D}(\mathcal{E}^\sharp)$. We want to estimate $\mathcal{E}^\sharp(f)$ from below by a sum of discrete energies. Set $I_n := V_n \cap I$, for $n \in \mathbb{N}$. For $n \in \mathbb{N}$ define:

$$\begin{aligned}f_n &:= H_{K_\sharp \setminus I_n}^{\mathcal{E}^\sharp} f,\\ d_0 &:= f_0,\\ d_{n+1} &:= f_{n+1} - f_n.\end{aligned} \tag{7.1}$$

Since f is continuous by [18, Theorem 4.14] it is even uniformly continuous on $K_\sharp$. Thus the minimum principle for harmonic functions applied to each element of $(f_n)_n$ tells us that f_n tends to f uniformly. Because of $f_n = \sum_{j=0}^n d_j$ this implies

$$f = \sum_{n=0}^{\infty} d_n. \tag{7.2}$$

We also have $\mathcal{E}^\sharp(f_n) = \mathcal{F}^\sharp_{n+k}(f_n)$, for all $n \in \mathbb{N}$, because $\mathcal{F}^\sharp_0$ is a $\Lambda^\sharp_\eta$-fixed point. The Gauss-Green formula for $\mathcal{F}^\sharp_{n+k}$ shows that $\mathcal{F}^\sharp_{n+k}(d_n, d_{n+k}) = 0$. Hence $\mathcal{E}^\sharp(d_n, d_{n+k}) = 0$. This implies $\mathcal{E}^\sharp(f_n) = \sum_{j=0}^n \mathcal{E}^\sharp(d_n)$ which converges to

$$\mathcal{E}^\sharp(f) = \sum_{n=0}^\infty \mathcal{E}^\sharp(d_n) = \sum_{n=0}^\infty \mathcal{F}^\sharp_n(d_n). \tag{7.3}$$

To identify the trace of $\mathcal{D}(\mathcal{E}^\sharp)$ on I we use Theorem 8.1 in the appendix. We see that, for $1/2 < \alpha < 1$, we have $f \in B^{2,2}_\alpha(I)$ if and only if

$$\|f\|_2 + \left(\sum_{n=0}^\infty 3^{n(2\alpha-1)} \sum_{k=1}^{3^n} |f(k3^{-n}) - f((k-1)3^{-n})|^2 \right)^{\frac{1}{2}} < \infty. \tag{7.4}$$

For $n \in \mathbb{N}$ denote by Δ^n_k the subtriangle of side length 3^{-n} whose corner points lie in I_n and comprise the points $k3^{-n}(1,0)$ and $(k-1)3^{-n}(1,0)$. Set

$$\mathcal{F}^\sharp_n(\Delta^n_k)(f) := \frac{1}{2} \sum_{x,y \in V_n \cap \Delta^n_k} (f(y) - f(x))^2 c_{\mathcal{F}^\sharp_n}(x,y).$$

Lemma 7.2 (C.f. [13, Cor. 4.3]) *There exists $\rho \in (0,1)$ such that for every nonconstant $f : V_1 \to \mathbb{R}$ which is $\mathcal{F}^\sharp_1$-harmonic on $V_1 \setminus V_0$,*

$$\sum_{i=1}^3 \mathcal{F}^\sharp_1(\Delta^1_i)(f) \le \rho \cdot \mathcal{F}^\sharp_1(f).$$

Proof. Consider the configuration in Figure 7. Suppose the dashed triangles are of the form Δ^1_k for $k = 0, 1, 2$. Then every nonconstant real valued function f on the vertices of Figure 7 defines a $0 \le \rho(f) \le 1$ by

$$\sum_{k=0}^3 \mathcal{F}^\sharp_1(\Delta^1_k)(f) =: \rho(f) \cdot \mathcal{F}^\sharp_1(f).$$

The forms in the above equation are homogeneous of degree 2 in f, so we can assume $\|f\|_2 = \sqrt{2}$. Furthermore, all forms vanish on constants, hence we may suppose that f is orthogonal to the constant function 1. When $0 < \rho(f) < 1$ on the resulting compact set of functions, then our assertion follows by continuity.

Since f is nonconstant, the irreducibility of $\mathcal{F}^\sharp_1$ implies $0 < \rho(f)$. Suppose $\rho(f) = 1$. Then the $\mathcal{F}^\sharp_1$-energy of f on the solid triangles of Figure 7 is 0 and f must be constant on these triangles. Let us denote the up most vertex in Figure 7 by z and the Dirichlet operator of $\mathcal{F}^\sharp_n$ by F_n, for $n = 0, 1$. Then $F_1 f(z) = 0$ and the self-similarity of $\mathcal{F}^\sharp_1$ implies $F_0 f(z) = 0$. Now the symmetries of F_0 in Lemma 7.1 show that $f(z) - f(a_0) = f(a_3) - f(z)$. Since F_0 and F_1 vanish on constants, we may thus assume $f(z) = 0$ and $f(a_0) = -f(a_3) = 1$. The mean value property of f in the vertex of Δ^1_2 which is different from a_2 and a_3 shows that $f(a_2) = 1$. A similar argument shows $f(a_1) = -1$. Thus the mean value property of f in a_2 is violated. In other words, f has to be constant when $\rho(f) = 1$. □

Theorem 7.3 (C.f. [13, Thm. 4.1]) *For $1 < \eta_C < 3$ the trace of $\mathcal{D}(\mathcal{E}^\sharp)$ on I is $B^{2,2}_\alpha(I)$, with $\alpha = \frac{1}{2} + \frac{\ln \eta_C}{\ln 9}$.*

Proof. Estimating (7.4) from above: For η_C as above, $b \in (0,\infty)^2$ as in Lemma 7.1 and $u \in \mathcal{D}(\mathcal{E}^\sharp)$ we have

$$\eta_C^n \cdot b \cdot |u(k3^{-n}(1,0)) - u((k-1)3^{-n}(1,0))|^2 \le \mathcal{F}^\sharp_n(\Delta^n_k)(u). \tag{7.5}$$

Let $m \in \mathbb{N} \setminus \{0\}$ and set $u = d_m$ on the left hand side of (7.5). Use Lemma 7.2 and $\mathcal{F}^\sharp_n(\Delta^m_k)(d_m) = \mathcal{E}^\sharp(\Delta^m_k)(d_m)$ to deduce

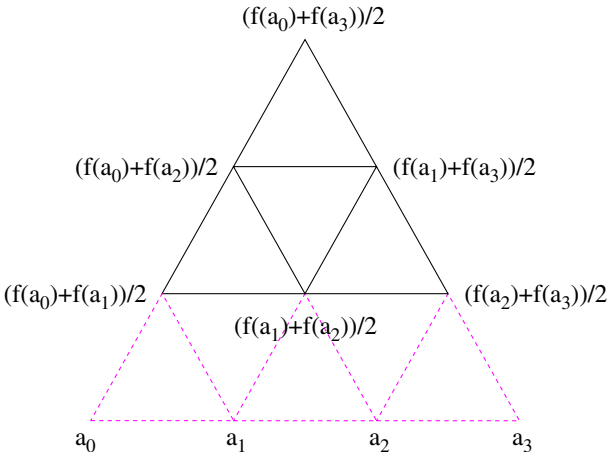

Fig. 7 (online colour at: www.mn-journal.org) The model configuration of the extension algorithm

$$\begin{aligned}\sum_{k=1}^{3^n} \eta_C^n \cdot b \cdot |d_m(k3^{-n}(1,0)) - d_m((k-1)3^{-n}(1,0))|^2 &\le \sum_{k=1}^{3^n} \mathcal{F}_n^\sharp(\Delta_k^n)(d_m) \\ &\le \sum_{k=1}^{3^m} \rho^{n-m} \mathcal{F}_n^\sharp(\Delta_k^m)(d_m) \\ &\le \rho^{n-m} \mathcal{E}^\sharp(d_m).\end{aligned}$$

Taking the square root on both sides of the above inequality and employing Minkowski's inequality we deduce

$$\begin{aligned}&\left(\sum_{k=1}^{3^n} |f_n(k3^{-n}(1,0)) - f_n((k-1)3^{-n}(1,0))|^2\right)^{1/2} \\ &\quad\le \left(\frac{\rho^n}{b\eta_C^n}\right)^{1/2} \sum_{m=0}^{n} \left(\rho^{-m}\mathcal{E}^\sharp(d_m)\right)^{1/2}.\end{aligned} \tag{7.6}$$

Now we use $\eta_C = 3^{2\alpha-1}$, $f = f_n$ on $V_n \cap I$ and (7.6) for the next inequality. Then Hardy's inequality in [19, Eq. 1'] gives the second inequality and, finally, (7.3) shows the last equality:

$$\begin{aligned}&\sum_{n=0}^{\infty} 3^{n(2\alpha-1)} \sum_{k=1}^{3^n} |f(k3^{-n}(1,0)) - f((k-1)3^{-n}(1,0))|^2 \\ &\quad\le \frac{1}{b} \sum_{n=0}^{\infty} \rho^n \left(\sum_{m=0}^{n} \left(\rho^{-m}\mathcal{E}^\sharp(d_m)\right)^{1/2}\right)^2 \\ &\quad\le \frac{4}{b(1-\rho)^2} \sum_{m=0}^{\infty} \rho^m \rho^{-m} \mathcal{E}^\sharp(d_m) \\ &\quad= \frac{4}{b(1-\rho)^2} \mathcal{E}^\sharp(f).\end{aligned}$$

Estimating the energy from above: Consider the configuration of points in Figure 7. Suppose $f(a_i)$ is given for $i = 0, \ldots, 3$. We extend f to the upper three triangles in Figure 7 as indicated. The corresponding unscaled conductances are defined by the T-triangle. So the energy is:

$$\frac{(f(a_0) - f(a_1))^2}{4} + \frac{(f(a_3) - f(a_2))^2}{4} + \frac{((f(a_0) - f(a_1)) + (f(a_2) - f(a_3))^2}{4},$$

$$\frac{(f(a_1)-f(a_2))^2}{4}+\frac{(f(a_3)-f(a_2))^2}{4}+\frac{((f(a_1)-f(a_2))+(f(a_2)-f(a_3)))^2}{4},$$
$$\frac{(f(a_0)-f(a_1))^2}{4}+\frac{(f(a_2)-f(a_1))^2}{4}+\frac{((f(a_0)-f(a_1))+(f(a_1)-f(a_2)))^2}{4}.$$

Using the convexity of $x \mapsto x^2$ we estimate their sum from above by

$$\frac{3}{2}\sum_{k=1}^{3}(f(a_k)-f(a_{k-1}))^2. \tag{7.7}$$

Let $f \in B^{2,2}_\alpha(I)$. We use the values of f in $a_k := k3^{-1}(1,0)$, $k = 0,1,2,3$, to prescribe values $Ef(\cdot)$ in the vertices of the upper 3 triangles of generation 1. Inside these triangles we extend $\mathcal{E}^\sharp$-harmonically. Thus the $\mathcal{E}^\sharp$-energy of the resulting function Ef on these three triangles is $\frac{15}{7}$ times the energy in (7.7). Suppose we have constructed Ef on all of $K_\sharp$ except in the subtriangles of generation n which intersect I. Each such subtriangle is subdivided into subtriangles of generation $n+1$. On each generation n triangle we extend as in Figure 7. The resulting energy of all subtriangles of generation n under consideration is

$$\frac{15}{7}\cdot\frac{3}{2}\cdot\eta_C^{n-1}\sum_{k=1}^{3^n}(f(k3^{-n}(1,0))-f((k-1)3^{-n}(1,0)))^2. \tag{7.8}$$

On subtriangles of generation n which intersect I we extend f as in Figure 7. Their conductances are given by the $\sharp$-triangles. So the scaled energy of all subtriangles of generation n which intersect I is

$$\eta_C^n\cdot\frac{2b+s}{2}\sum_{k=1}^{3^n}(f(k3^{-n}(1,0))-f((k-1)3^{-n}(1,0)))^2. \tag{7.9}$$

The sum of (7.8) and (7.9) shows that we can bound $\mathcal{E}^\sharp(Ef)$ from above by a constant multiple of the double sum in (7.4). □

8 Appendix

According to [14, Prop. 1 on p. 114] the classical norm in $B^{2,2}_\alpha(I)$, $0<\alpha<1$, is equivalent to

$$\|f\|_B := \|f\|_2+\left(\sum_{n=0}^{\infty}L^{n(1+2\alpha)}\iint_{|x-y|<L^{-n}}|f(y)-f(x)|^2\,dx\,dy\right)^{1/2} \tag{8.1}$$

for $L=2$. By [24, Lemma 2] every $L\geq 2$ defines an equivalent norm. We intend to show that this norm is equivalent to

$$\|f\|_D := \|f\|_2+\left(\sum_{n=0}^{\infty}L^{n(2\alpha-1)}\sum_{k=1}^{L^n}|f(kL^{-n})-f((k-1)L^{-n})|^2\right)^{\frac{1}{2}}. \tag{8.2}$$

Interpreting I as a fractal with Hausdorff dimension 1 we can use [14, Cor. 2 on p. 214] to deduce that $B^{2,2}_\alpha(I)$ is continuously embedded into $\mathrm{Lip}(\alpha-1/2,I)$, that is, its functions are Hölder continuous if $1/2<\alpha<1$.

Theorem 8.1 *Let $L\in\mathbb{N}\setminus\{0,1\}$. On $C(I,\mathbb{R})$, $\|\cdot\|_B$ and $\|\cdot\|_D$ are equivalent.*

Proof. For $L=2$ this is [15, Thm. 1.1]. Our proof will rely almost entirely on the proof of Theorem 5 in [24]. Again we have to interpret I as a nested fractal.

For the convenience of the reader we switch to the notation of [24]: $N=1$ because $I=[0,1]\subset\mathbb{R}^N$, $L\geq 2$ because we contract I by $1/L$ each time we apply a similitude, $M=L$ because we subdivide I into L subintervals, $\mathcal{K}=I$ is our fractal, $V_0=\{0,1\}$ because our subintervals overlap in their boundary points, $V_n=\{kL^{-n}\mid 0\leq k\leq L^n\}$ is the n-th refinement of I, $d_f(\mathcal{K})=1$ because the Hausdorff dimension of

I is 1, $\mathcal{F}_n = \{kL^{-n} + [0, L^{-n}] \mid 0 \le k < L^n\}$ are the subintervals of length L^{-n}, μ_n is the normalized counting measure of V_n and μ is the (one dimensional) Lebesgue measure, the conductances $(a_{xy})_{x,y\in V_0}$ are just $(a_{01}) = (1)$, the energy of generation 0 then is $\mathcal{E}^{(0)}(f,f) = (f(1) - f(0))^2$, the energy scaling factor is $\rho = L$, the unscaled energy of generation n hence is

$$\tilde{\mathcal{E}}^{(n)}(f,f) = \frac{1}{2} \sum_{\substack{x,y\in V_n \\ |x-y|=L^{-n}}} (f(y) - f(x))^2,$$

the dimension of the walk is $d_w = 2$,

$$b_n(f) = L^{n\alpha} \left(L^n \iint_{|x-y|<L^{-n}} (f(y) - f(x))^2 \, dx \, dy \right)^{1/2},$$

$c_0 = 1$ because it is the length of I, and, finally, $k = k_0 = 1$ on page 283 and 285 because $L^{d_f}/L^{d_w} = 1/L < 1/2$ for $L > 2$. We also use c as a generic constant which might change its finite value in every inequality.

We firstly bound $\|\cdot\|_B$ by a multiple of $\|\cdot\|_D$. Every function under consideration is continuous. Thus we can replace the Lebesgue measure μ by the counting measure μ_n and consider the weak limit for $n \to \infty$. The arguments on the pages 279–281 show that for $n \ge m$,

$$\begin{aligned}
&\iint_{|x-y|<L^{-m}} (f(y) - f(x))^2 \, d\mu_n(x) \, d\mu_n(y) \\
&\quad \le c \cdot \frac{L^{n-m}}{L^{2n}} \sum_{r=m}^{n-1} 2^{r-m+1} L^{n-(r+1)} \tilde{\mathcal{E}}^{(r+1)}(f,f) \\
&\quad = c \cdot L^{-2m} \sum_{r=0}^{n-m-1} \left(\frac{2}{L}\right)^{r+1} \tilde{\mathcal{E}}^{r+m+1}(f,f).
\end{aligned}$$

Now letting n tend to infinity, multiplying both sides by $L^{m(1+2\alpha)}$ and summing over m we arrive at

$$(\|f\|_B - \|f\|_2)^2 \le c \cdot \sum_{m=0}^{\infty} L^{m(2\alpha-1)} \sum_{r=0}^{\infty} \left(\frac{2}{L}\right)^{r+1} \tilde{\mathcal{E}}^{r+m+1}(f,f).$$

All terms of the above sum are positive. So we can rearrange them. The factor of $\tilde{\mathcal{E}}^m(f,f)$ is

$$\sum_{k=0}^{m-1} L^{k(2\alpha-1)} \left(\frac{2}{L}\right)^{m-k+1}.$$

When it can be bounded from above by a multiple of $L^{m(2\alpha-1)}$, then the desired estimate follows. Such a bound exists if and only if the following sum is uniformly bounded in m.

$$\sum_{k=0}^{m-1} \left(L^{2\alpha-1}\right)^{k-m} \left(\frac{2}{L}\right)^{m-k} = \left(\frac{2}{L^{2\alpha}}\right)^m \frac{1 - \left(\frac{L^{2\alpha}}{2}\right)^m}{1 - \frac{L^{2\alpha}}{s}} = \frac{2}{L^{2\alpha}} \cdot \frac{\left(\frac{2}{L^{2\alpha}}\right)^m - 1}{\frac{2}{L^{2\alpha}} - 1}.$$

This is the case if and only if $2 < L^{2\alpha}$, that is, $\frac{1}{2}\frac{\ln 2}{\ln L} < \alpha$. So $1/2 < \alpha$ is sufficient.

Next we want to bound $\|\cdot\|_D$ from above by a multiple of $\|\cdot\|_B$. The arguments on the pages 281–284 of [24] show that

$$\begin{aligned}
\tilde{\mathcal{E}}^{(m)}(g,g) &\le c(g) L^m L^{(m+\nu)(-1)} \\
&\quad + cL^m \sum_{r=0}^{\nu-1} 2^{r+2} 3^{m+2r+1} \int_{\mathcal{K}} \int_{|p-q|<L^{-(m+r)}} (g(p) - g(q))^2 \, d\mu(p) \, d\mu(q).
\end{aligned}$$

For $\nu \to \infty$ and a different constant c this shows

$$\tilde{\mathcal{E}}^{(m)}(g,g) \le cL^{2m} \sum_{r=0}^{\infty} \left(\frac{2}{L^2}\right)^r \int_{\mathcal{K}} \int_{|p-q|<L^{-(m+r)}} (g(p)-g(q))^2 \, d\mu(p)\, d\mu(q).$$

Multiplying both sides by $L^{m(2\alpha-1)}$ and summing over m yields

$$\begin{aligned}&(\|f\|_D - \|f\|_2)^2 \\ &\quad \le c \sum_{m=0}^{\infty} L^{m(2\alpha+1)} \sum_{r=0}^{\infty} \left(\frac{2}{L^2}\right)^r \int_{\mathcal{K}} \int_{|p-q|<L^{-(m+r)}} (g(p)-g(q))^2 \, d\mu(p)\, d\mu(q).\end{aligned}$$

Again all terms of the above sum are positive and we calculate the factor of $\int_{\mathcal{K}} \int_{|p-q|<L^{-m}}$. It can be bounded from above by a multiple of $L^{m(2\alpha+1)}$ if and only if the following sum is uniformly bounded in m.

$$\sum_{k=0}^{m} L^{(k-m)(2\alpha+1)} \left(\frac{2}{L^2}\right)^{m-k} = \left(\frac{2}{L^{2\alpha+3}}\right)^m \sum_{k=0}^{m} \left(\frac{L^{2\alpha+3}}{2}\right)^k.$$

This is the case if and only if $2 < L^{2\alpha+3}$, that is, $-1 < \alpha$ suffices. □

Acknowledgements Both authors gratefully acknowledge the support by the START-project Y96-MAT of the Austrian Science Foundation. The first author was additionally supported by the DFG research group "Spektrale Analysis, asymptotische Verteilungen und stochastische Dynamik".

References

[1] W. N. Anderson and G. E. Trapp, Shorted operators, II, SIAM J. Appl. Math. **28** (1), 60–71 (1975).
[2] J. Bliedtner and W. Hansen, Potential Theory. An Analytic and Probabilistic Approach to Balayage (Springer, Berlin, 1986).
[3] P. G. Doyle and J. L. Snell, Random Walks and Electrical Networks, Carus Mathematical Monographs Vol. 22 (Math. Assoc. America, Washington, D.C., 1984).
[4] G. A. Edgar, Measure, Topology, and Fractal Geometry (Springer, New York, 1990).
[5] G. A. Edgar, Integral, Probability, and Fractal Measures (Springer, New York, 1998).
[6] K. J. Falconer, Fractal Geometry. Mathematical Foundations and Applications (Wiley, Chichester, 1990).
[7] M. Fukushima, Y. Oshima, and M. Takeda, Dirichlet Forms and Symmetric Markov Processes, de Gruyter Studies in Mathematics Vol. 19 (de Gruyter, Berlin – New York, 1994).
[8] B. M. Hambly, Brownian motion on a homogeneous random fractal, Probab. Theory Related Fields **94** (2), 1–38 (1992).
[9] B. M. Hambly and T. Kumagai, Diffusion processes on fractal fields: heat kernel estimates and large deviations, Probab. Theory Related Fields **127**, 305–352 (2003).
[10] B. M. Hambly and S. O. G. Nyberg, Finitely ramified graph directed fractals, spectral asymptotics and the multidimensional renewal theorem, Proc. Roy. Soc. Edinburgh Sect. A **46**, 1–34 (2002).
[11] T. Hattori, H. Hattori, and H. Watanabe, Gaussian field theories on general networks and the spectral dimension, Progr. Theoret. Phys. Suppl. **92**, 108–143 (1987).
[12] A. Jonsson, Dirichlet forms and Brownian motion penetrating fractals, Potential Anal. **13**, 69–80 (2000).
[13] A. Jonsson, A trace theorem for the Dirichlet form on the Sierpinski gasket, Research Reports, No. 8, Department of Mathematics, Umeå University (2003).
[14] A. Jonsson and H. Wallin, Function Spaces on Subsets of $\mathbb{R}^n$, Mathematical Reports 2, Part 1 (Harwood Academic Publ., London, 1984).
[15] A. Kamont, A discrete characterization of Besov spaces, Approx. Theory Appl. (N.S.) **13**, 63–77 (1997).
[16] J. Kigami, Analysis on Fractals, Cambridge Tracts in Mathematics Vol. 143 (Cambridge Univ. Press, Cambridge, 2001).
[17] T. Kumagai, Brownian motion penetrating fractals. An application of the trace theorem of Besov spaces, J. Funct. Anal. **170**, 69–92 (2000).
[18] S. Kusuoka, Diffusion processes on nested fractals, in: Statistical Mechanics and Fractals, edited by R. L. Dobrushin and S. Kusuoka, Lecture Notes in Mathematics Vol. 1567 (Springer, Berlin – Heidelberg, 1993), pp. 39–98.
[19] L. Leindler, Generalization of inequalities of Hardy and Littlewood, Acta Sci. Math. (Szeged) **31**, 279–285 (1970).

[20] T. Lindstrøm, Brownian motion penetrating the Sierpinski gasket, in: Asymptotic Problems in Probability Theory, Stochastic Models and Diffusions on Fractals, edited by K. D. Elworthy and N. Ikeda (Longman Scientifc, Harlow, 1993), pp. 248–278.
[21] R. D. Mauldin and S. C. Williams, Hausdorff dimension in graph directed constructions, Trans. Amer. Math. Soc. **309**, 811–829 (1988).
[22] V. Metz, How many diffusions exist on the Vicsek snowflake?, Acta Appl. Math. **32**, 227–241 (1993).
[23] V. Metz, The Short-cut Test, J. Funct. Anal. **220**, No. 1, 118–156 (2005).
[24] K. Pietruska–Paluba, Some function spaces related to the Brownian motion on simple nested fractals, Stoch. Stoch. Rep. **67**, 267–285 (1999).
[25] H. Triebel, Fractals and Spectra related to Fourier Analysis and Function Spaces, Monographs in Mathematics Vol. 91 (Birkhäuser, Basel, 1997).

